ORIGINAL ARTICLE

Parametric analyses of dynamic interaction between three-dimensional soil and frame structure group under earthquake loadings

Jishuai Wang[1] · Tong Guo[1] · Yazhou Xie[2] · Zhenyu Du[1]

Abstract

Dynamic interaction between soil and structure group (SSGI) is of great significance to the seismic design and evaluation of structures in densely built areas. However, detailed three-dimensional parametric analysis of the SSGI effect using realistic modeling on both the superstructure and soil is still limited. This study develops a three-dimensional numerical method to account for the SSGI effect and validates it against the shaking table test result. Subsequently, parametric analyses are conducted to investigate the SSGI effect for a three-dimensional soil and structure group, where key parameters include the structure height, number, and spacing, material properties of the soil, and spectrum distributions of seismic records. Compared with the dynamic interaction between soil and a single structure, the SSGI can reduce the structural base shear and story drift (up to 17% and 24%, respectively) in most cases. However, the level of reduction is below 5% when (1) structure spacing is greater than 2.0 times the width of the structure foundation or (2) the shear wave velocity of soil is no less than 300 m/s. Essentially, the SSGI changes the seismic demand of the concerned structure mainly by altering its local ground acceleration input at the base. The SSGI effect is more significant when structure spacing is reduced, structure number is increased, or the height of the central structure equals those of the surrounding structures. In contrast, the influence of soil property on the SSGI effect is minor under medium-level earthquakes.

Keywords Soil–structure group interaction · Structure–soil–structure interaction · Parametric analysis · Three-dimensional · Finite element method

✉ Tong Guo
    guotong@seu.edu.cn

1   School of Civil Engineering, Southeast University, 2 Sipailou, Nanjing 210096, People's Republic of China

2   Department of Civil Engineering, McGill University, 817 Sherbrooke Street West, Montreal H3A 0C3, Canada

1 Introduction

In recent years, the influence of dynamic interaction between soil and structure group (SSGI) on the seismic demands of structures has received increased attention due to the enhanced requirement of seismic risk mitigation in densely built areas. The SSGI effect on structural seismic demands tends to be more significant in the bustling areas of over-populated cities because most building groups are composed of a large number of buildings, and the separation distances between buildings are relatively small. The SSGI is also termed structure-soil-structure dynamic interaction (SSSI) (Knappett et al. 2015), an extension of soil-structure interaction (SSI) and is more complex than SSI. Material properties of subsoil, dynamic characteristics of the structure, and uncertainties in ground motions are essential factors influencing SSI. In addition to these factors, SSGI is also affected by the structures' number, height, spacing, plane arrangements, etc. Because of the fruitful research outcomes in the past [e.g., (Housner. 1957; Bielak 1975; Stewart et al. 1999; Alkaz and Zaicenco 2007; Lin and Miranda 2008)], the SSI effect has recently been included in the seismic design codes across the globe [e.g., (MHURD-PRC 2010a; NBCC 2010; IBC 2012)]. However, compared with SSI, research on SSGI is limited; it is also often neglected or substantially simplified when regionwide buildings are of concern (Lu et al. 2018; Zhang et al. 2021). As a result, it remains unknown to what degree the seismic demands of buildings in densely built areas would be affected by SSGI.

Luco and Contesse (1973) first investigated the SSSI effect regarding the interaction of two shear walls with rigid foundations subjected to incident antiplane shear (SH) waves on a half-space. Afterwards, Wong and Trifunac (1975) studied the two-dimensional SH-type vibration of several shear walls with rigid foundations embedded in an elastic, homogeneous half-space. These studies indicated that (1) the SSSI effect was prominent at low frequencies and frequencies close to the natural frequencies of the adjacent structures; (2) smaller and lighter structures were more easily affected by their neighbors; and (3) the motion observed at the structural base could be quite different from the free-field ground motion. Subsequently, studies on site-city dynamic interaction (SCI) were conducted (Clouteau and Aubry 2001; Guéguen et al. 2002; Isbiliroglu et al. 2015; Guéguen and Colombi 2016) to examine the dynamic interaction effect between building clusters and supporting soils on the city scale. These studies focused on investigating the effect of SCI on the ground motions and seismic demands of individual structures in the context of regionwide seismic wave propagation. However, most of these studies treated soils as an infinite half-space or an idealized (trapezoidal) basin on a half-space. The buildings therein have also been simplified as single degree of freedom (SDOF) structures, or simplified solid columns, without considering their rocking behaviors or soil embedments of foundations.

Recent efforts have been made to investigate the SSGI effects for better assessing and designing structures or structural members in densely built areas. Padron et al. (2009, 2011) studied the dynamic through-soil interaction between pile-supported structures in a viscoelastic half-space under incident S and Rayleigh waves. They addressed the SSGI effect on the responses of piles that support several building groups with different configurations. Bybordiani and Arici (2019) studied the dynamic interaction between plane soil and adjacent buildings by using the substructure method to combine the building models with layered soils. Wang and Zhang (2021) investigated the influence of various influencing factors on the interaction effect between elastic soil and two or more buildings based on the three-dimensional FEM. In addition to pure numerical studies, a few experimental

investigations on the SSGI effect have also been conducted. Aldaikh et al. (2016) studied the dynamic interaction between a foam block and two or three SDOF structures subjected to five real seismic records, finding that compared with the structure only considering SSI, the presence of adjacent structures could increase or reduce seismic power and acceleration responses of structure. Ge et al. (2019) conducted shaking table tests on the dynamic interaction between scaled clay soil and a structure group composed of five SDOF structures by employing the El Centro wave and Shanghai wave, pointing out that the SSGI could reduce the structural acceleration responses and increase or reduce the structural velocity responses compared with SSI. Wang et al. (2022a) and Du et al. (2022) carried out a series of shaking table tests on scaled soil-structure group systems with different configurations and validated the significant influence of SSGI on the structural seismic responses and local ground motion characteristics under earthquake loadings. Compared with other experiments, the test of Wang et al. (2022a) captured the significant influence of interaction between soft soil and structure groups with different plane arrangements and structure numbers on the structural acceleration responses. All previous experimental investigations indicated that the presence of adjacent structures could positively or negatively change the structural seismic responses, and its influence was different when facing different seismic records.

Existing studies on the SSGI effect achieve useful conclusions but have certain limitations. For instance, most of the structures considered in these studies were highly simplified (e.g., two-dimensional plane frames or SDOF models) and could not capture the irregularity or higher vibration modes of real-world buildings. Besides, the SSGI effect on the maximum story drift (a significant seismic demand), cannot be obtained when simplifying superstructures to the SDOF structures (Wang et al. 2022a, 2022b). In addition, there lacks comprehensive investigations of all factors that are potentially influential to the SSGI effect. In response to these concerns, the SSGI effect is thoroughly investigated in the current study by using three-dimensional FEM with more realistic considerations of superstructures and soils. In particular, a three-dimensional FEM able to account for the SSGI effect is developed and validated by shaking table test results. Thereafter, the numerical parametric analyses on the SSGI effect are conducted to evaluate the influences of several key parameters, including structure height, spacing, number, and arrangement, material properties of soil, and spectrum distributions of seismic records. It is found that the SSGI effect can reduce the structural base shear and story drift in most cases compared with SSI. By changing the local ground acceleration input at the structure base, the SSGI effect is more significant when structure spacing is small, structure number is large, soil shear wave velocity is small, and the height of the central structure equals those of the surrounding structures.

2 Numerical model and its validation against shaking table tests

A three-dimensional numerical model is developed using the software platform of ABAQUS for accounting for the SSGI effect. As shown in Fig. 1, beams, columns, and piles are simulated by Beam31 elements, and the roofs, floors, and pile caps are simulated by S4R shell elements. The soil boundaries are simulated by a series of artificial dashpots connected to the ground; the soil is modeled by C3D8 elements; the seismic excitations are realized through inputting time-history accelerations to the bottom boundary of soils. The constitutive model of the soil is selected as the equivalent linear model (Martin and Seed
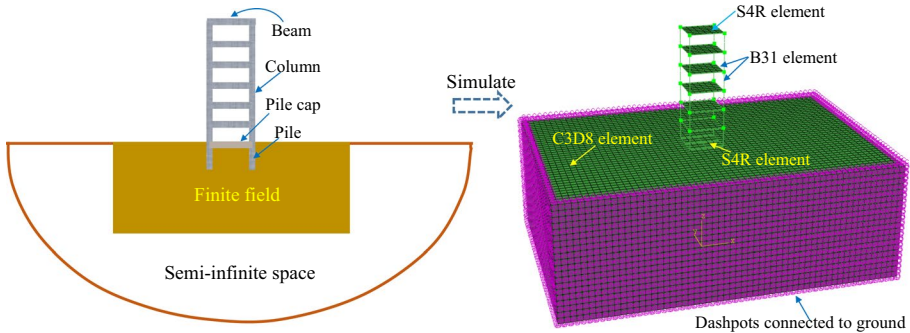
Fig. 1 Schematic illustration of the numerical model

1982), which assumes the soil to be a viscoelastic medium. In particular, the equivalent linear model characterizes the shear stiffness and energy dissipation capacity of soil using the dynamic shear modulus (G_d) and damping ratio (D), respectively. Equations (1) and (2) show the closed-form formulae for computing G_d and D, where γ_d and G_{max} denote the dynamic shear strain and maximum dynamic shear modulus of soil, respectively; A, B, γ_0, D_{max} and β are coefficients obtained by regressing the empirical models against soil test results, such as those from the dynamic triaxial test. Since the equivalent linear model is not precise under large soil shear strains (i.e., when subjected to strong ground shaking), this study investigates the SSGI effect under medium-level earthquakes. Besides, the structural nonlinearity is neglected, and the soil and piles are fully coupled by referring to Ge et al. (2019) for improved computational efficiency. The above setting is applied not only to the validation of the numerical model, but also to all subsequent parametric analyses.

$$\frac{G_d}{G_{max}} = 1 - \left\{ \frac{(\gamma_d/\gamma_0)^{2B}}{1 + (\gamma_d/\gamma_0)^{2B}} \right\}^A \tag{1}$$

$$\frac{D}{D_{max}} = \left(1 - \frac{G_d}{G_{max}} \right)^\beta \tag{2}$$

Shaking table test results (Wang et al. 2022a) are utilized to verify the effectiveness of the above numerical model. The shaking table test uses a scaled test specimen with the similarity ratios of density, elastic modulus, and length (S_ρ, S_E, and S_l) determined as 1:1.5, 1:6, and 1:20, respectively. The size, density, and shear wave velocity of the scaled soil are 2.9 m×2.0 m×1.25 m, 1.1 ton/m^3, and 60 m/s, and those of prototype soil are 58 m×40 m×25 m, 1.65 ton/m^3, and 120 m/s, respectively. The scaled soil is placed in a laminated container (Bhattacharya et al. 2012; Tabatabaiefar 2016; Tsai et al. 2016; Fiorentino et al. 2021) with a plane clear size of 2.9 m×2.0 m. The mass and lateral stiffness of the hypothetical prototype SDOF structure are 158.4 tons and 24,988 kN/m, respectively. The scaled SDOF structure is shown in Fig. 2a, where the SDOF structure is made of a steel pipe with a mass block attached to the top; the mass of the mass block is 13.2 kg, and the internal and external diameters of the steel pipe are 0.04 m and 0.045 m. The pile foundation of the hypothetical prototype SDOF structure is composed of a pile cap with a plane size of 6 m×6 m, and four piles with a length and diameter of 8 m and 0.8 m. The

(a) Soil-single-structure system   **(b)** Soil-5-structure system   **(c)** Soil-11-structure system

Fig. 2 Field photos of shaking table tests (Wang et al 2022a)

pile foundation of scaled SDOF structure consists of a steel pile cap with a plane size of 0.3 m×0.3 m, and four steel piles with a length and diameter of 0.4 m and 0.04 m, respectively. The G_{max} of the scaled soil is 3.6 MPa, and the coefficients A, B, γ_0, D_{max}, and β in Eqs. (1) and (2) are calibrated as 1.141, 0.320, 0.00230, 0.238, and 0.796, respectively, for the tested soil. The field photos of the shaking table tests are shown in Fig. 2 for three cases. In Soil-5-structure and Soil-11-structure systems, the clear spacing between buildings is 0.5L, where L denotes the width of the pile foundation.

The finite element models of the Soil-single-structure, Soil-5-structure, and Soil-11-structure systems are established for carrying out the dynamic time-history analyses. The input ground motion is selected as a scaled seismic record Taft with a peak acceleration of 140 cm/s^2 and a time interval of 0.001 s (Wang et al 2022a). Figure 3 compares the numerical and experimental results in both time-histories and Fourier spectra for the accelerations at the top of the central structure in the Soil-single-structure system. A good agreement can be observed in Fig. 3 regarding the peak accelerations and maximum Fourier amplitudes between simulated and tested results. Likewise, the peak accelerations of the structures at the center for the Soil-single-structure, Soil-5-structure, and Soil-11-structure systems are further compared in Fig. 4. The numerical results show consistent trends versus test outcomes—namely, the acceleration demands of the central structure decrease with a larger structure number. The above comparisons indicate that the numerical model for the Soil-SDOF structure group system is reliable. The superstructure is the only difference between the Soil-SDOF structure group system and the Soil-frame structure group system. Considering that the adopted modeling method of frame structure has been widely used and validated [e.g., (Wang 2020; Zhang and Far 2021)], the presented numerical model for the Soil-frame structure group system can be applied to account for the SSGI effect and used in the subsequent parametric analyses.
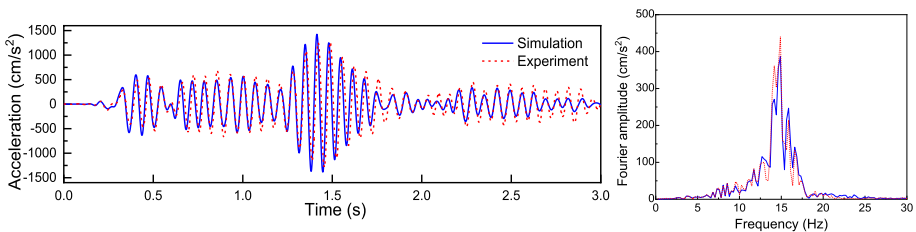

Fig. 3 Comparisons between experimental and simulated results in time-histories and Fourier spectra for the accelerations at the top of the central structure in the Soil-single-structure system
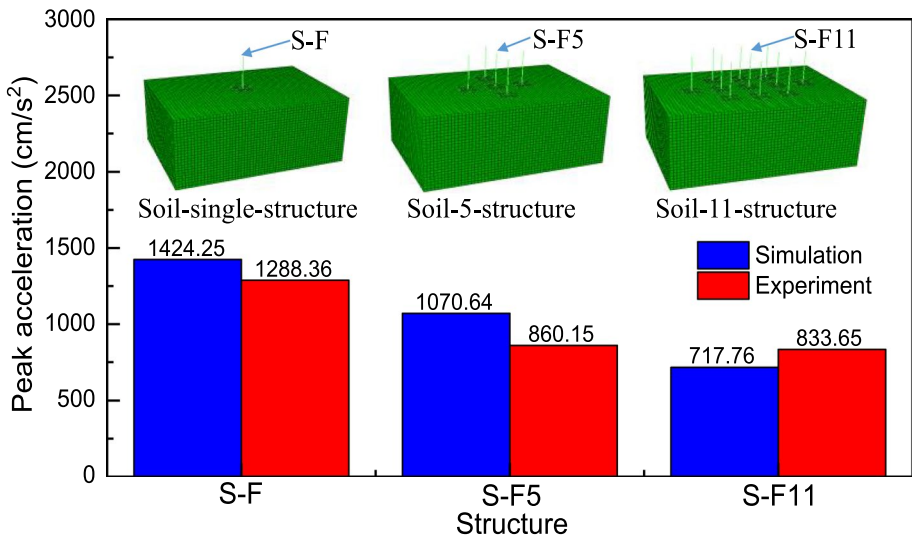
Fig. 4 Comparisons of test and simulated results of peak accelerations at the top of central structures

3 Influence of structure height, soil shear wave velocity, and spectrum distributions of seismic records

3.1 Parameter consideration and model setup

Considering the wide use of reinforced concrete frames (RC-frames) worldwide, the dynamic interactions between homogeneous soil and pile-supported RC-frame groups are investigated. As shown in Fig. 5, the influence of structure height is examined by considering hypothetical pile-supported RC-frames with 3, 6, 9, 12, and 15 stories. The width and story height of all RC-frames are 6 m and 3.3 m; their foundations are designed as
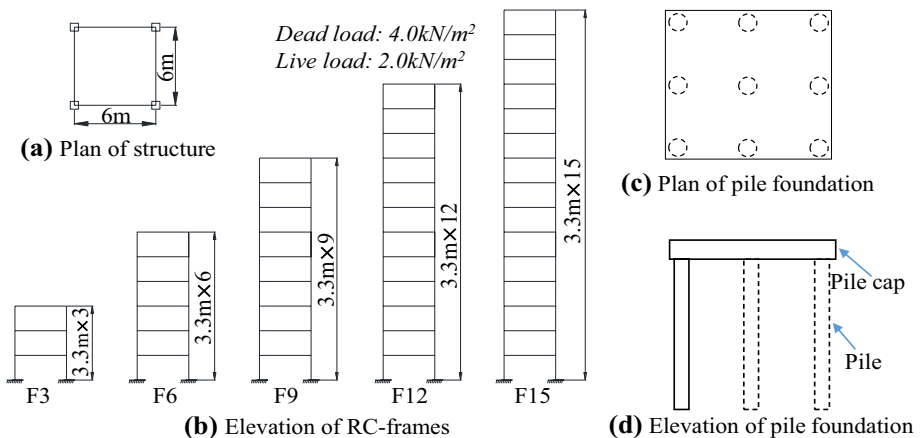

Fig. 5 Plan and elevations of RC-frames and the diagram of pile foundation

the 3×3 pile foundation. Moreover, the nomenclatures and detailed geometric parameters of the RC-frames are shown in Table 1. Besides, both the foundation and frame adopt the C35 grade concrete with the elastic modulus of 32,500 MPa (MHURD-PRC 2010b). The foundation scheme presented in Table 1 is applied to all soil conditions considering that the influence of pile length and diameter on the SSGI effect is limited (Wang and Zhang 2021). In engineering practice, detailed pile design should be conducted to examine, for instance, soil bearing capacity, and select the appropriate pile foundation under each distinct soil condition. Modal analyses on the fixed-base RC-frames reveal that the periods of F3, F6, F9, F12, and F15 frames are 0.380, 0.731, 1.112, 1.511, and 1.927 s, respectively.

The shear wave velocities of soils range from 100 to 500 m/s to cover soil conditions at most building sites and comprehensively investigate their influence on the SSGI effect. The numerical model set the soil thicknesses as 20 m by referring to MHURD-PRC (2010a), as well as the plane size to be 58 m in length and 40 m in width. The length and width of the soil medium are greater than $5.0L$, which can minimize the boundary effect in the finite element analysis (Han et al. 2013); this plane size is considered sufficient to capture the SSGI effect on the central structure. Furthermore, due to the high computational cost for running the 3D high-fidelity FEMs that cover a broad spectrum of influential parameters, six seismic records with distinctly different spectral characteristics are selected from the PEER Ground Motion Database and the peak accelerations of them are scaled to the same value, so as to adequately investigate the influence of spectral characteristics of seismic records on the SSGI effect. The selected motions' key information are presented in Table 2, whereas their Fourier spectra with the peak acceleration of 1.0 cm/s^2 are shown in Fig. 6. These seismic records are ground accelerations recorded at the surfaces of soils. As such, seismic deconvolution analyses are conducted using code SHAKE (Schnabel 1972) to obtain the corresponding motion records at the bedrocks, which are subsequently used as the bottom inputs for the dynamic time-history analyses of different soil-structure systems.

The clay soil is adopted herein as the benchmark case, while the influences of different soil types will be presented in Sect. 5. The shear modulus reduction (G/G_{max}) curve and the damping ratio (D) curve of the clay soil, and the associated coefficient parameters for the equivalent linear model are presented in Fig. 7. Figure 8 presents the developed ten finite element models for the comparative study. Five models in Fig. 8(a) consider one building

Table 1 Detailed parameters of RC-frames with pile foundations

Structures	Superstructures			Pile foundations	
	Story	Beam (mm)	Column (mm)	Pile diameter (mm)	Pile Length (mm)
F3	1 to 3	300×600	500×500	300	2000
F6	1 to 6	300×600	600×600	450	4000
F9	1 to 5	300×600	650×650	550	6000
	6 to 9	300×600	550×550		
F12	1 to 4	300×600	700×700	650	8000
	5 to 8	300×600	600×600		
	9 to 12	300×600	500×500		
F15	1 to 5	300×600	750×750	750	10,000
	6 to 10	300×600	650×650		
	11 to 15	300×600	550×550		

Table 2 Ground motion records

| Records	Earthquake name	Year	Station name	Magnitude	Rjb (km)	Component
RSN-587	New Zealand-02	1987	Matahina Dam	6.6	16.09	A-MAT083.AT2
RSN-1108	Kobe_ Japan	1995	Kobe University	6.9	0.9	KBU000.AT2
RSN-1750	Northwest China-02	1997	Jiashi	5.93	17.9	JIA000.AT2
RSN-79	San Fernando	1971	CIT Athenaeum	6.61	25.47	PAS000.AT2
RSN-136	Santa Barbara	1978	Santa Barbara Court-house	5.92	0	SBA222.AT2
RSN-1050	Northridge-01	1994	Pacoima Dam	6.69	4.92	PAC175.AT2

Fig. 6 Fourier spectra of seismic records
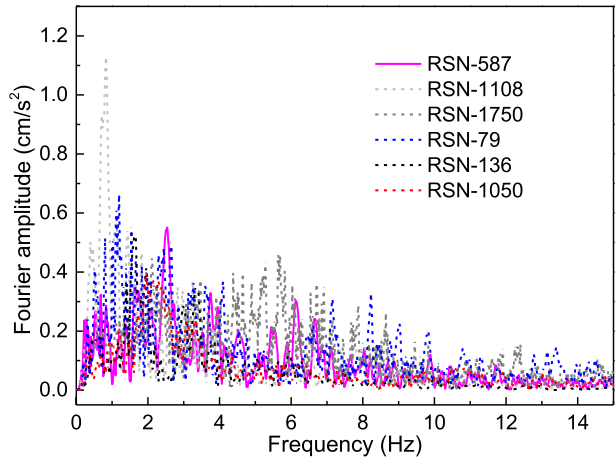
Fig. 7 Material parameters of the clay soil
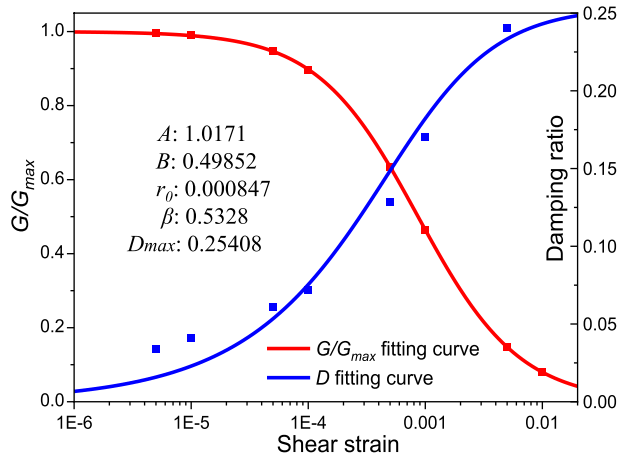
only to engage the SSI effect. In contrast, five additional models are built in Fig. 8b, each including nine buildings at a spacing of 0.5L. The development of these multi-building finite element models aims to investigate the SSGI effect. The peak accelerations of the three seismic records are scaled to 100 cm/s², and the corresponding bedrock records are

(a) SSI systems
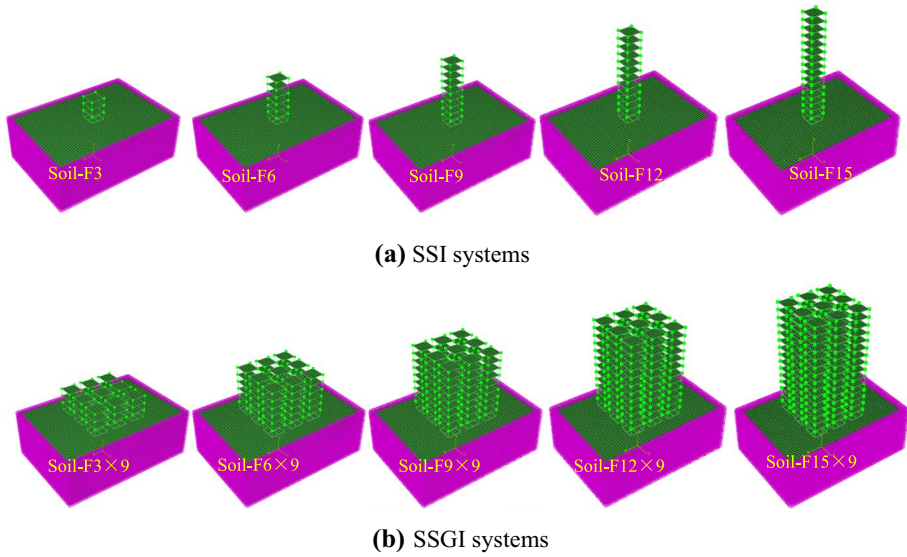

(b) SSGI systems

Fig. 8 Finite element models of SSI systems and SSGI systems

obtained through seismic deconvolution analyses. Seismic responses of these different soil-structure systems are obtained by inputting the bedrock motions to the bottom boundaries of the models.

3.2 Performance metrics to quantify the SSGI effect

The SSGI effect is assessed as the relative impact due to the existence of adjacent buildings. As such, the SSGI effects on the maximum story drift and base shear of the target structure are quantified using E_{sd} and E_{bs}:

$$E_{sd} = \frac{G_{sd} - S_{sd}}{S_{sd}} \tag{3}$$

$$E_{bs} = \frac{G_{bs} - S_{bs}}{S_{bs}} \tag{4}$$

where S_{sd} and S_{bs} denote the maximum story drift and base shear of the structures in SSI systems, which only included one structure (i.e., those in Fig. 8a); G_{sd} and G_{bs} represent the maximum story drift and base shear of the central structures in SSGI systems (i.e., those in Fig. 8b).

3.3 Analysis results of the SSGI effect

The values of E_{bs} and E_{sb} under different seismic records, structure heights, and soil shear wave velocities are computed. As shown in Figs. 9 and 10, the structure height, soil shear wave velocity, and spectrum distribution of seismic records all have significant effects on
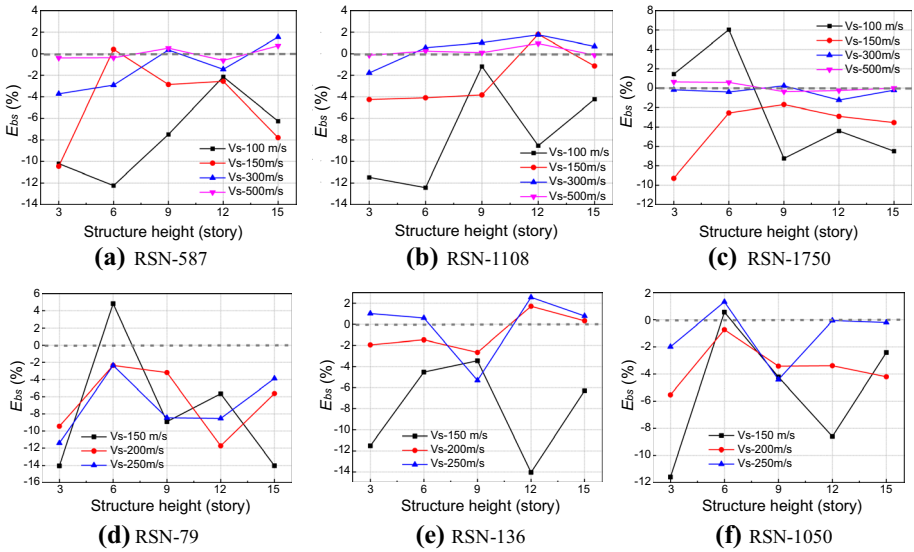
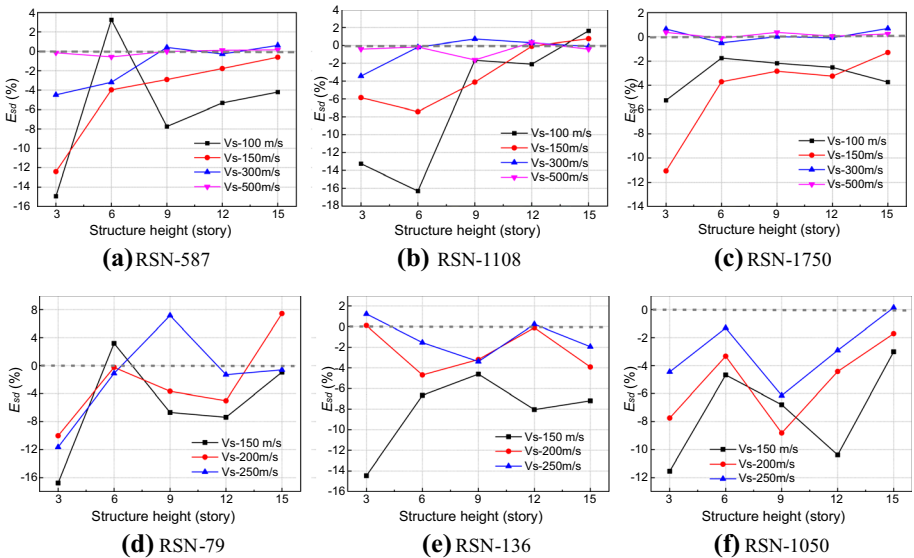**Fig. 9** Comparison of curves for E_{bs} under different seismic records

Fig. 10 Comparison of curves for E_{sd} under different seismic records

E_{bs} and E_{sb} when the V_s is less than 300 m/s, indicating that the influence on the SSGI effect should fully consider the above three factors when the structure group is located at soft soils (i.e., $V_s < 300$ m/s). Conversely, it can be observed that the values of E_{bs} and E_{sd} are respectively less than 4% and 5% when V_s is no less than 300 m/s, indicating that as compared with SSI, the effect of SSGI on structural seismic demands is somewhat negligible

when stiff soils support the groups of structures. Moreover, it is found that the E_{bs} and E_{sd} show distinct curve trends under the same seismic record when the V_s is between 100 and 150 m/s. Such different curve trends between Figs. 9 and 10 represent that the influence of SSGI on the maximum base shear is not proportional to that on the maximum story drift compared with SSI. The reason could be that the presence of adjacent structures changes the vibration mode of the target structure during earthquakes. Besides, it is found that, in general, SSGI tends to be more significant under soft soil conditions for structure groups with smaller heights. As adjacent structures are much stiffer than the supporting soils, they significantly affect the central structure's responses. In addition, the SSGI can reduce the structural base shear and story drift in most cases compared with SSI. This is because the SSGI can significantly reduce Fourier amplitudes for acceleration at the base of the target structure in most cases, which will be discussed in detail in Sect. 4. Conversely, SSGI can also increase the seismic demands of the structure in some specific cases compared with SSI. One such specific case is investigated in detail below.

As shown in Fig. 9c, the E_{bs} for F6 is about 6% when the V_s is 100 m/s and the seismic record is RSN-1750. This represents that the base shear of F6 in the Soil-F6×9 system is 6% greater than that of F6 in the Soil-F6 system. The seismic response of the building considering SSI is expected to be mainly affected by the acceleration at the base of the structure and the rocking response of the foundation. Therefore, the Fourier spectra and 5%-damping pseudo acceleration spectra of accelerations at the base of the F6 in Soil-F6 and Soil-F6×9 systems are compared in Fig. 11a, b. Besides, the vertical accelerations of points at the edge of the pile cap for F6 in Soil-F6 and Soil-F6×9 systems are compared
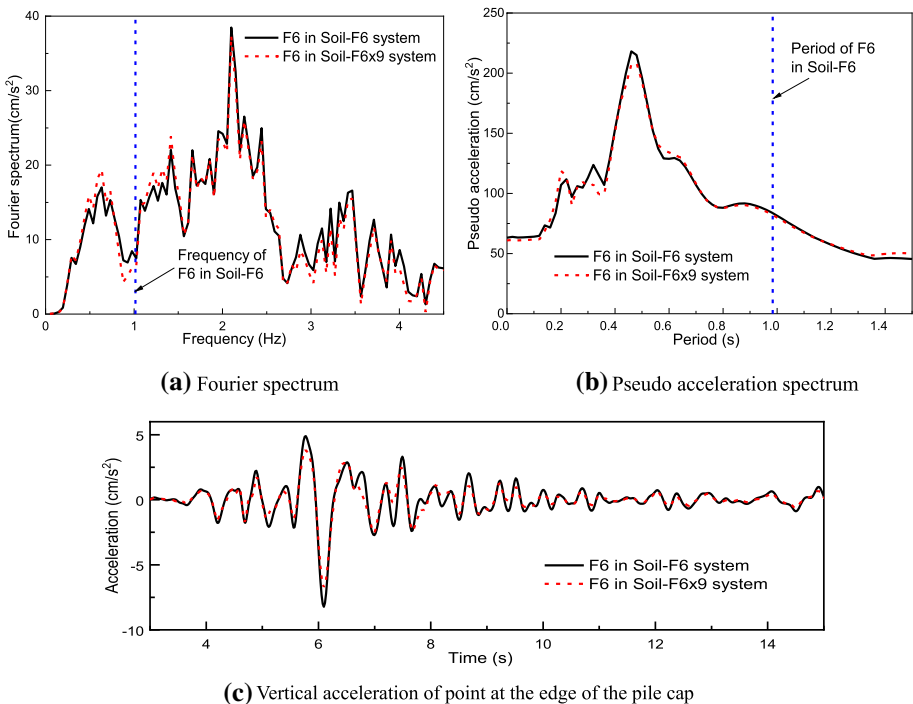

(a) Fourier spectrum   (b) Pseudo acceleration spectrum

(c) Vertical acceleration of point at the edge of the pile cap

Fig. 11 Comparisons of Fourier spectra, pseudo spectra, and vertical accelerations

in Fig. 11c. These vertical accelerations are positively correlated with the rocking motions of building foundations. It is observed from Fig. 11a that the Fourier amplitudes of the structural base acceleration increase at some frequencies and decrease at other frequencies after considering SSGI, resulting in that the pseudo acceleration of F6 at its natural period somewhat does not change between SSI and SSGI, as shown in Fig. 11b. However, Fig. 11c shows that the vertical acceleration at one edge of the pile cap for F6 is significantly reduced (up to 18.5% at the peak point) after considering SSGI, indicating that the SSGI, in this case, would constrain the rocking motion of the F6 building. Therefore, the SSGI herein increases the base shear of F6 because adjacent structures further limit the rocking motion of its foundation.

4 Influence of structure spacing and structure number

4.1 Structure spacing

The plane size of soil is extended to 58 m×56 m, and the structure spacing of the nine-building case is set as 0.17L, 0.5L, 1.0L, 1.5L, and 2.0L, respectively, to investigate the influence of structure spacing on SSGI. The values of E_{bs} and E_{sd} under different structure heights, seismic records, and shear wave velocities are shown in Fig. 12. In general, the influence of structure spacing on the SSGI effect is coupled with those from structure height, spectrum distribution of seismic records, and shear wave velocity of soil. The SSGI could decrease the maximum base shear and story drift of the central structures by about 17% and 24%, respectively, when the structure spacing is 0.17L. In contrast, the SSGI effect on the responses of RC-frames is mitigated with larger structure spacing, and both E_{bs} and E_{sd} would reduce to within 4% when the structure spacing reaches 2.0L. Therefore, it is recommended to ignore the SSGI effect when structure spacing is greater than 2.0L. The physics behind the above finding is that the input energy of scattered waves caused by vibrations of adjacent structures is absorbed by the soil when being propagated to the concerned structure. The soil absorbs more energy when the structure spacing is larger, resulting in less disturbance on the seismic demands of the concerned structure.

Likewise, the Fourier spectra and 5%-damping pseudo acceleration spectra of accelerations at the bottom of the central structures for Soil-F3×9 systems with structure spacing at 0.17L, 0.5L, and 1.0L are compared in Fig. 13a, c. As a representative case, the seismic record is chosen as the RSN-587 motion, and the soil shear wave velocity V_s is considered 150 m/s. To facilitate the comparisons, Fig. 13b, d also present
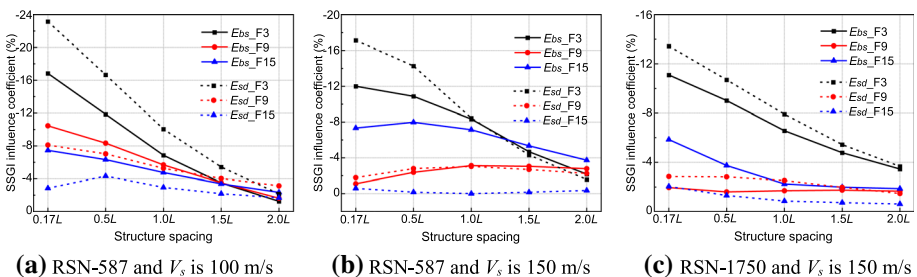

(a) RSN-587 and V_s is 100 m/s   **(b)** RSN-587 and V_s is 150 m/s   **(c)** RSN-1750 and V_s is 150 m/s

Fig. 12 Comparisons of the influences of structure spacing on SSGI

(a) Fourier spectrum

(b) Relative difference of Fourier amplitude

(c) Pseudo acceleration spectrum

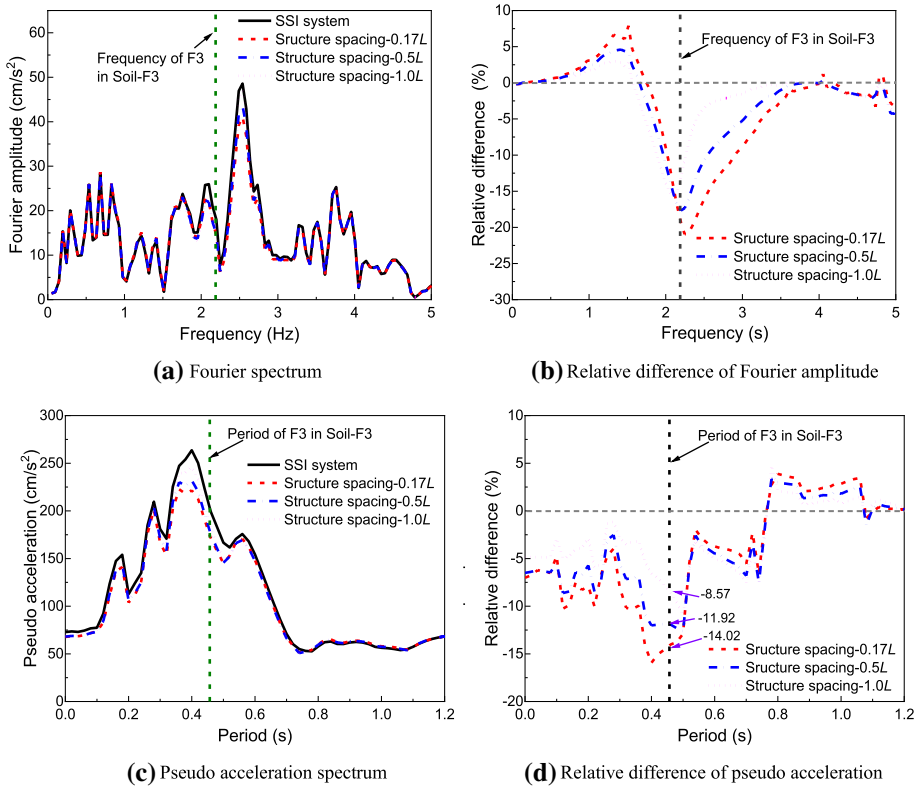**(d)** Relative difference of pseudo acceleration

Fig. 13 Comparisons of the influence of structure spacing on accelerations at the base of F3

the relative differences of these spectra values when compared with those for the SSI systems at all frequencies. Figure 13b indicates that the SSGI can significantly reduce the Fourier amplitudes at frequencies near the frequencies of adjacent structures; this reduction decreases with larger structure spacing. Due to resonance, adjacent structures exhibit strong movements at frequencies close to their natural frequency. Such strong movements show more significant influences on the acceleration at the base of the target structure. This finding can explain the influence of structure spacing on the pseudo acceleration spectra of accelerations at the bottom of central structures in Soil-F3 × 9 systems, as shown in Fig. 13c, d.

In addition, it can be seen from Fig. 13d that, compared with SSI, the base shear forces of the central structures in Soil-F3 × 9 systems with structure spacing of 0.17L, 0.5L, and 1.0L are reduced by 14.02%, 11.92%, and 8.57%, respectively. Besides, the actual reductions in base shear forces are 12.01%, 10.88%, and 8.34%, as shown in Fig. 12b. The estimated reductions in base shear obtained from the accelerations at the bottom of central structures are very close to the actual values, indicating that the SSGI changes the maximum base shear of the concerned structure mainly through changing its acceleration at the bottom.
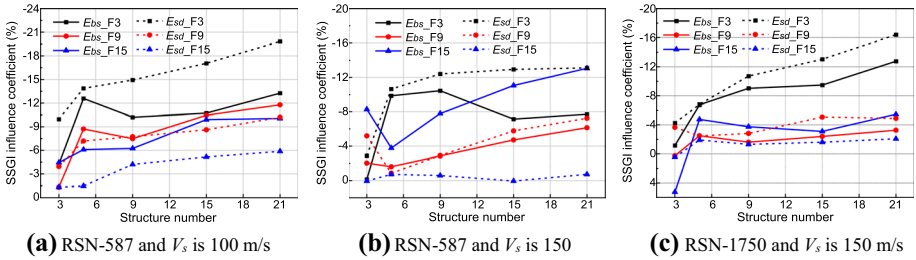
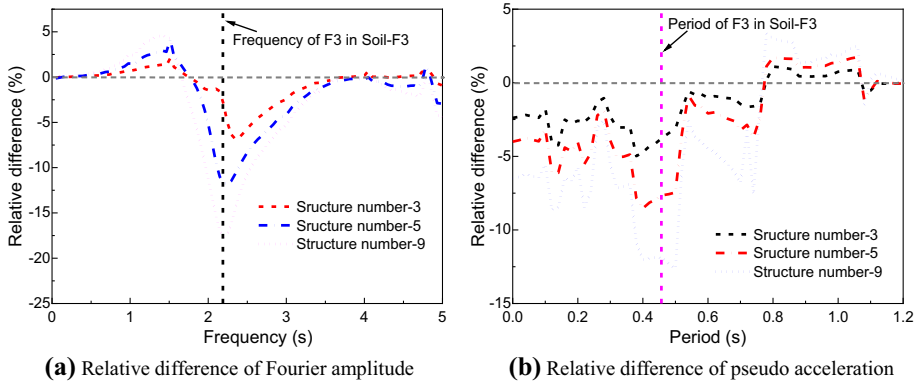**Fig. 14** Comparison of the influence of structure number

Fig. 15 Comparisons of the influence of structure number on accelerations at the bottom of F3

4.2 Structure number

The structure numbers of RC-frame groups are set as 3, 5, 9, 15, and 21, respectively, to study their influence on the SSGI. The structure spacing is considered 0.5L for all cases. The values of E_{bs} and E_{sd} under different structure heights, seismic records, and soil shear wave velocities are shown in Fig. 14. It is found that, in general, the SSGI effect on the responses of RC-frames increases with a larger number of structures. Similarly, the influences of structure number on the SSGI effect are coupled with those from structure height, spectrum distribution of seismic records, and shear wave velocity of soil. The SSGI effect on the maximum base shear and story drift of the central structures shows the maximum values of about 13% and 20%, respectively, for the 21 building case, when the buildings have three stories and are supported by soft soils ($V_s = 100$ m/s) (Fig. 14a).

Similar to the analysis regarding structure spacing, the relative differences in the Fourier spectra and pseudo acceleration spectra of accelerations at the bottom of the central structures in Soil-F3×3, Soil-F3×5, and Soil-F3×9 systems compared with the Soil-F3 system are shown in Fig. 15a, b. It can also be observed that the SSGI significantly reduces the Fourier amplitudes at the frequencies near the frequency of adjacent structures. Such reductions decrease when fewer structures are considered, as a larger number of adjacent structures would influence the local ground acceleration for the central structure more substantially. The reason is that vibrations of a larger
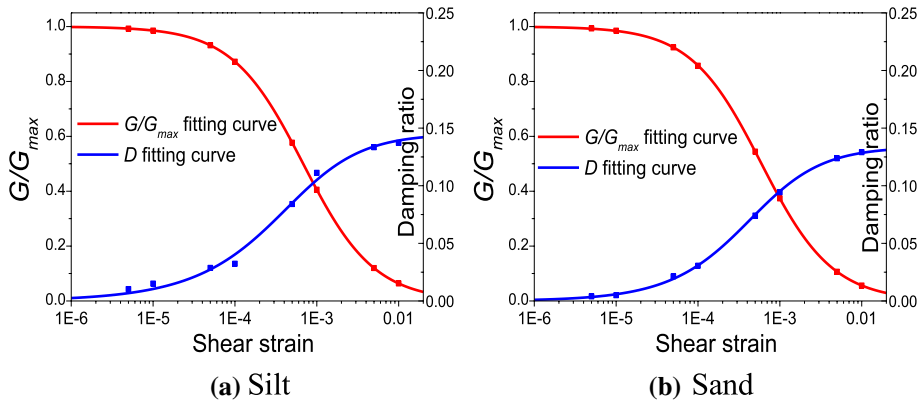
(a) Silt　　　　**(b)** Sand

Fig. 16 Fitting curves of dynamic shear modulus ratio and damping ratio

Table 3 Material parameters of silt and sand

Soil type	Fitting parameters				
	A	B	r_0	D_{max}	β
Silt	0.999	0.500	0.000683	0.145	0.622
Sand	1.024	0.498	0.000578	0.134	0.754

number of adjacent structures generate more scattered waves and propagate more wave energy to the concerned structure, producing more disturbance on the local ground acceleration of the concerned structure.

5 Influence of soil type and structure group's plane arrangement

5.1 Soil type

Three common types of soil, namely clay, silt, and sand, are considered herein to investigate the influence of soil type on the SSGI effect. Dynamic triaxial tests have been conducted to identify the shear modulus reduction (G/G_{max}) and the damping ratio (D) at different shear strains of these soils, as given in Figs. 7 and 16 (Yuan et al. 2000). Moreover, nonlinear regression analyses are conducted to obtain the fitting curves (Fig. 16) and the corresponding parameter coefficients (Table 3) using Eqs. (1) and (2).

In this section, the record RSN-587 with the peak acceleration of 100 cm/s^2 is considered, and the structure number, spacing, and shear wave velocity of soil are selected as 9, 0.5L, and 150 m/s, respectively. The values of E_{bs} and E_{sd} under different soil types and structure heights are shown in Fig. 17a, b, respectively. It is observed that the maximum differences on E_{bs} and E_{sd} by considering a distinct soil type are only 1.89% and 2.16%, respectively. The soil type bears a negligible impact on the SSGI effect when the peak acceleration of the ground motion is 100 cm/s^2.
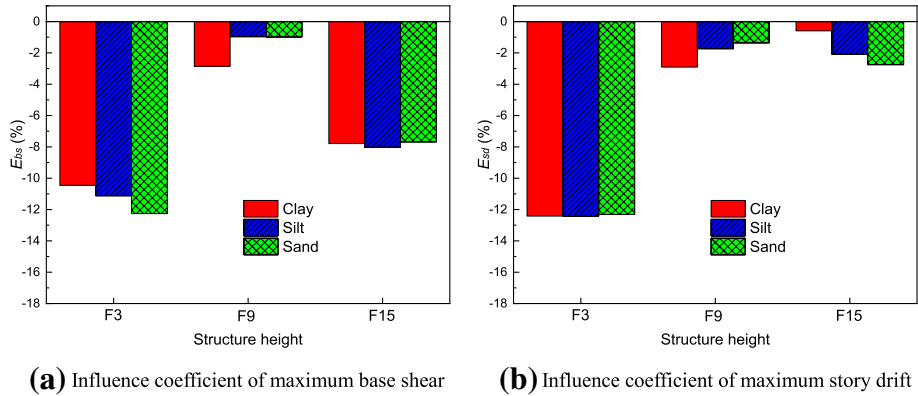
(a) Influence coefficient of maximum base shear   (b) Influence coefficient of maximum story drift

Fig. 17 Comparisons of the influence of soil type on the SSGI effect

5.2 Structure group's plane arrangement

The height and plane arrangement of surrounding structures might also affect the SSGI effect. To investigate the height effect, Soil-F3×5, Soil-F3-F15×4, Soil-F9×5, Soil-F9-F3×4, Soil-F15×5, and Soil-F15-F3×4 systems are established as shown in Fig. 18. The soil shear wave velocity in these systems is selected as 150 m/s, and motion records RSN-587 and RSN-1750 with peak accelerations of 100 cm/s^2 are applied as the seismic excitations. The values of E_{bs} and E_{sd} in different SSGI systems are also compared in Fig. 18. In general, the SSGI effect is more significant when the central structure's height equals those of the surrounding structures. This phenomenon was also captured in the shaking table test of dynamic interaction between soft soil and structure group (Wang et al. 2022a). The physics behind the above finding is that the dominant frequencies of
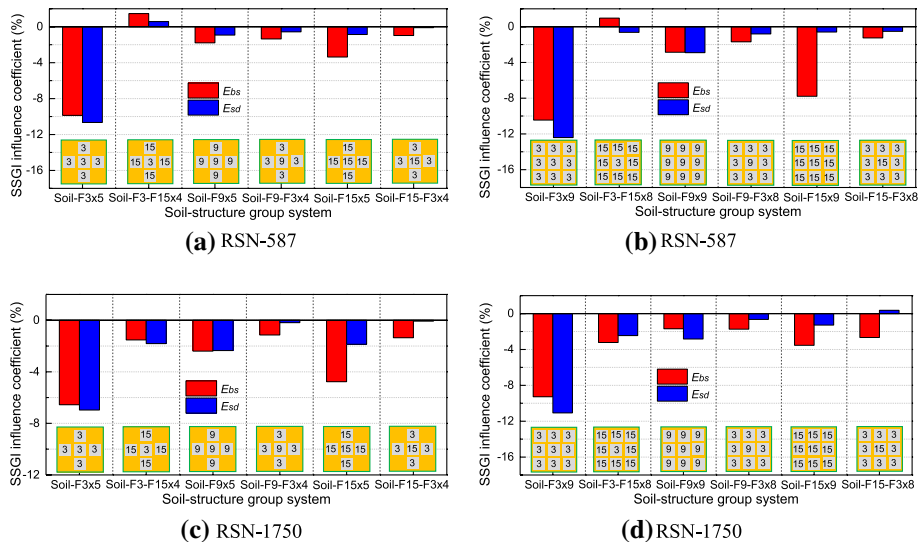

(a) RSN-587   (b) RSN-587

(c) RSN-1750   (d) RSN-1750

Fig. 18 Comparisons of SSGI effects under structure groups with different structures

scattered waves caused by vibrations of adjacent structures are close to the frequencies of adjacent structures, and the resonance effect occurs when the concerned structure's frequency equals those of adjacent structures. Besides, it is found that the influence of SSGI becomes lower than 4% when different heights are designed between the central and surrounding structures. When the dynamic properties of adjacent structures differ significantly from those of the central structures, adjacent structures only have minor influences on the local ground acceleration of the central structure. This phenomenon is because the change in pseudo acceleration of acceleration at the base of the target structure reaches the maximum at natural frequencies of adjacent structures, as discussed in Sect. 4.

As shown in Fig. 19, Soil-F3×3, Soil-F3×3-V, Soil-F9×3, Soil-F9×3-V, Soil-F15×3, Soil-F15×3-V, Soil-F3×5, Soil-F3×5-H, Soil-F9×5, Soil-F9×5-H, Soil-F15×5, Soil-F15×5-H systems are established, respectively, to examine the influence of structure group arrangement on the SSGI effect. In these cases, the soil shear wave velocity V_s is selected as 150 m/s, whereas the same normalized seismic records RSN-587 and RSN-1750 are applied as the ground motion inputs. The values of E_{bs} and E_{sd} in SSGI systems with different plane arrangements are also compared in Fig. 19. Both positive and negative values are pinpointed from the figure; the values of E_{bs} and E_{sd} are also affected by structure heights and input ground motions under the same plane arrangement. In particular, the comparisons in Fig. 19 indicate that SSGI effect can be significantly influenced by the structure group's plane arrangement in some specific cases.

The relative differences in the Fourier spectra of accelerations at the bottom of the central structures in Soil-F3×5-H and Soil-F3×5 systems compared with those from the Soil-F3 system are explored in detail in Fig. 20a. The motion record RSN-587 is chosen as the ground motion excitation. Likewise, the same comparisons for the pseudo acceleration spectra of accelerations 0at the bottom of the central structures are shown in Fig. 20b. Figure 20a shows that the plane arrangement of the Soil-F3×5 system has a more significant effect on the acceleration at the bottom of the central structure when compared with the one for the Soil-F3×5-H system. Both these two plane arrangements tend to reduce the base shear of F3, as observed in Fig. 20b. However, Fig. 19b rather indicates that the E_{bs}
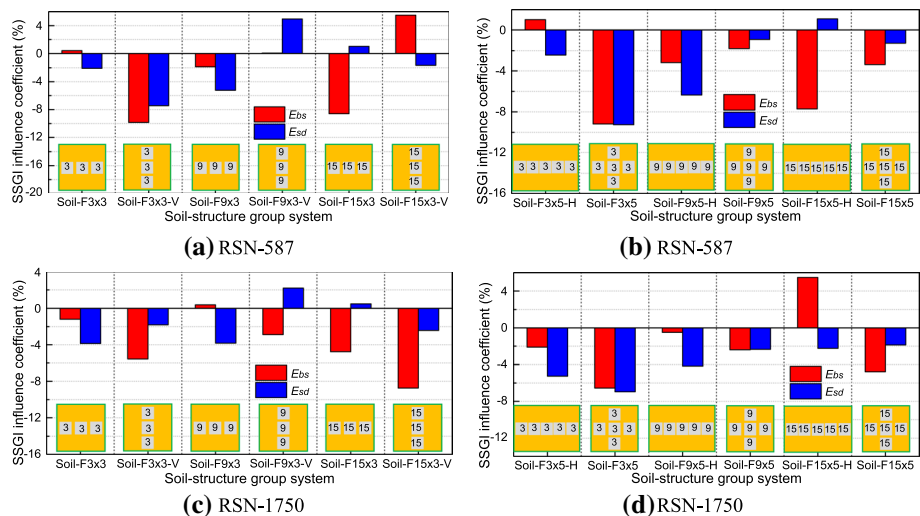

Fig. 19 Comparisons of SSGI effects under structure groups with different arrangements
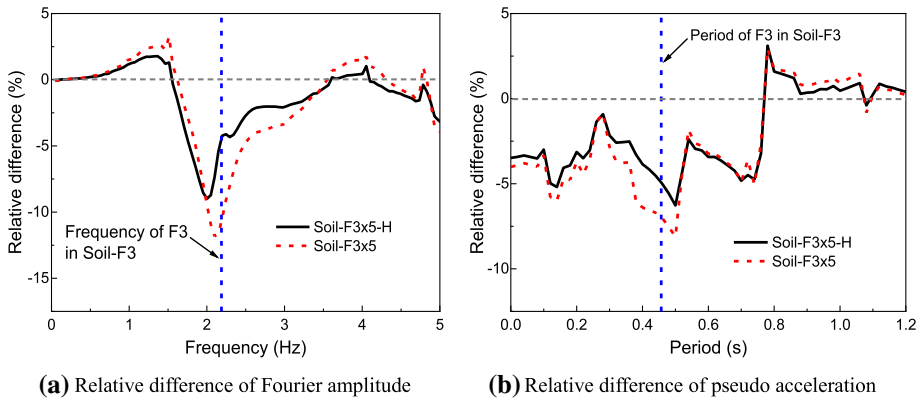
(a) Relative difference of Fourier amplitude   (b) Relative difference of pseudo acceleration

Fig. 20 Comparisons of the influence of plane arrangement on accelerations at the bottom of F3

for the Soil-F3×5 system is about −10%, while the E_{bs} is slightly greater than zero for the Soil-F3×5-H system. One essential difference between Figs. 19b and 20b lies in that the pseudo acceleration spectra in Fig. 20b neglect any potential rocking motions of the structure. Therefore, reliable evaluations of the SSGI effect cannot be achieved by only considering the local ground motion for the structure of concern, that is, the influence of SSGI on the rocking motions also needs to be properly quantified.

6 Conclusions

This study explores the SSGI effect through comprehensive parametric analyses using realistic numerical modeling on RC building frames and three-dimensional supporting soils. The influence of structure height, number, spacing, spectrum distributions of seismic records, and material properties of soils is investigated in depth. The following conclusions can be drawn from the current study based on the presented work.

1. SSGI can significantly reduce the Fourier amplitudes of accelerations at the base of concerned structures near the natural frequencies of adjacent structures. The level of reduction increases when structure spacing is small and structure number is large. Compared with SSI, the SSGI effect on the seismic demands of the central structure is within 4% when structure spacing is greater than 2.0L.
2. In most cases, the SSGI effect can reduce the structural base shear and story drift; its influence on the base shear is not proportional to that on the story drift. SSGI is more significant when short, stiff structures are supported by soft soils. Compared with SSI, the SSGI effect is within 5% when the shear wave velocity of soil is no less than 300 m/s; soil type bears negligible influence on the SSGI effect when subjected to medium-level earthquake events. Compared with the SSGI effect under the medium-level earthquake, the SSGI effect under a strong earthquake could increase or reduce, depending on mutually-coupled influential factors such as structure height, soil shear wave velocity, etc.
3. The SSGI effect is significant when the height of the central structure equals those of the surrounding structures. The structure plane arrangement changes the SSGI effect

both positively and negatively by altering not only the base input motion but also the rocking motions of the structure.

4. The SSGI changes the maximum base shear of the concerned structure mainly through changing its local ground acceleration input. However, the reliable evaluation of the SSGI effect on structural seismic demands cannot be achieved by only examining the local ground motion input; the influence of SSGI on the rocking motions also needs to be properly considered.

5. This paper conducts detailed parametric analyses on the interaction effect between equivalent linear soil and elastic structure groups under medium-level earthquakes. However, many issues such as the interaction effect between nonlinear soil and structure group under strong earthquakes, the SSGI effect on damage patterns, methods to quantify the SSGI effect, etc., still need to be solved through ongoing studies of the authors.

Statements and Declarations

Competing interests The authors have no relevant financial or non-financial interests to disclose.

References

Aldaikh H, Alexander NA, Ibraim E et al (2016) Shake table testing of the dynamic interaction between two and three adjacent buildings (SSSI). Soil Dyn Earthq Eng 89:219–232

Alkaz V, Zaicenco A (2007) Soil–structure interaction effects on an instrumented building. B Earthq Eng 5:533–547

Bhattacharya S, Lombardi D, Dihoru L, Dietz MS, Crewe AJ, Taylor CA (2012) Model container design for soil-structure interaction studies. Role of seismic testing facilities in performance-based earthquake engineering 135–158

Bielak J (1975) Dynamic behaviour of structures with embedded foundations. Earthq Eng Struct Dyn 3:259–274

Bybordiani M, Arici Y (2019) Structure–soil–structure interaction of adjacent buildings subjected to seismic loading. Earthq Eng Struct D 48:731–748

Clouteau D, Aubry D (2001) Modifications of the ground motion in dense urban areas. J Comput Acoust 9(04):1659–1675

Du Z, Guo T, Wang J, Yu S, Liu J, Liu X, Shen C (2022) Experimental and analytical study on ground motion characteristics under structure cluster disturbance. Earthq Eng Struct D 51(10):2267–2291

Fiorentino G, Cengiz C, De Luca F, Mylonakis G, Karamitros D, Dietz M, Nuti C (2021) Integral abutment bridges: investigation of seismic soil-structure interaction effects by shaking table testing. Earthq Eng Struct D 50(6):1517–1538

Ge Q, Xiong F, Xie L, Chen J, Yu M (2019) Dynamic interaction of soil–structure cluster. Soil Dyn Earthq Eng 123:16–30

Guéguen P, Bard PY, Chávez-García FJ (2002) Site-city seismic interaction in Mexico city—like environments: an analytical study. Bull Seismol Soc Am 92(2):794–811

Guéguen P, Colombi A (2016) Experimental and numerical evidence of the clustering effect of structures on their response during an earthquake: a case study of three identical towers in the city of Grenoble, France. Bull Seismol Soc Am 106(6):2855–2864

Han X, Xiao C, Yin J (2013) Dynamic elastoplastic analysis of interaction system of composite foundation-raft-superstructure under earthquake action. Rock Soil Mech 3:762–768 (**in Chinese**)

Housner GW (1957) Interaction of building and ground during an earthquake. Bull Seismol Soc Am 47:179–186

IBC (2012) International building code. International Code Council (ICC)

Isbiliroglu Y, Taborda R, Bielak J (2015) Coupled soil–structure interaction effects of building clusters during earthquakes. Earthq Spectra 1:463

Knappett JA, Madden P, Caucis K (2015) Seismic structure–soil–structure interaction between pairs of adjacent building structures. Geotechnique 65(5):429–441

Lin YY, Miranda E (2008) Kinematic soil-structure interaction effects on maximum inelastic displacement demands of SDOF systems. Bull Earthq Eng 6(2):241–259

Luco JE, Contesse L (1973) Dynamic structure–soil–structure interaction. Bull Seismol Soc Am 63:1289–1303

Lu X, Tian Y, Wang G, Huang D (2018) A numerical coupling scheme for nonlinear time history analysis of buildings on a regional scale considering site-city interaction effects. Earthq Eng Struct D 47(13):2708–2725

Martin PP, Seed HB (1982) One-dimensional dynamic ground response analyses. J Geotech Eng Div 108(7):935–952

MHURD-PRC (Ministry of Housing and Urban-Rural Development of the People's Republic of China) (2010a) "Code for seismic design of buildings." GB 50011-2010a, Beijing **(in Chinese)**

MHURD-PRC (Ministry of Housing and Urban-Rural Development of the People's Republic of China) (2010b) Code for design of concrete structures. GB 50010-2010b, Beijing **(in Chinese)**

National Building Code of Canada (NBCC) (2010) NRC Institute for Research in Construction, Canada

Padrón LA, Aznárez JJ, Maeso O (2009) Dynamic structure–soil–structure interaction between nearby piled buildings under seismic excitation by BEM–FEM model. Soil Dyn Earthq Eng 29(6):1084–1096

Padrón LA, Aznárez JJ, Maeso O (2011) 3-D boundary element–finite element method for the dynamic analysis of piled buildings. Eng Anal Bound Elem 35(3):465–477

PEER (Pacific Earthquake Engineering Research) (2014) PEER ground motion database. Accessed 15 Aug 2020. https://ngawest2.berkeley.edu

Schnabel PB (1972) SHAKE: a computer program for earthquake response analysis of horizontally layered sites. EERC Report 72-12, University of California, Berkeley

Stewart JP, Seed RB, Fenves GL (1999) Seismic soil–structure interaction in buildings. II : empirical findings. J Geotech Geoenviron 125(1):38–48

Tabatabaiefar HR (2016) Detail design and construction procedure of laminar soil containers for experimental shaking table tests. Int J Geotech Eng 10(4):328–336

Tsai C-C, Lin W-C, Chiou J-S (2016) Identification of dynamic soil properties through shaking table tests on a large saturated sand specimen in a laminar shear box. Soil Dyn Earthq Eng 83:59–68

Wang HF, Zhang RL (2021) Dynamic structure-soil-structure interaction of piled high-rise buildings under earthquake excitations II: influence of key parameter. Lat Am J Solids Stru 18(3):1–25

Wang J, Guo T, Du Z, Yu S (2022a) Shaking table tests and parametric analysis of dynamic interaction between soft soil and structure group. Eng Struct 256:114041

Wang J, Guo T, Du Z (2022b) Experimental and numerical study on the influence of dynamic structure–soil–structure interaction on the responses of two adjacent idealized structural systems. J Build Eng, 104454

Wong HL, Trifunac MD (1975) Two-dimensional, antiplane, building-soil-building interaction for two or more buildings and for incident plane SH waves. Bull Seismol Soc Am 65:1863–1885

Wang W (2020) Strain rate effect on the progressive collapse analysis of RC frame structure under earthquake. Adv Civ Eng

Yuan X, Sun R, Sun J, Meng S, Shi Z (2000) Laboratory experimental study on dynamic shear modulus ratio and damping ratio of soils. Earthq Eng Eng Vib 20(4):133–139 **(in Chinese)**

Zhang B, Xiong F, Lu Y, Ge Q, Liu Y, Mei Z, Ran M (2021) Regional seismic damage analysis considering soil–structure cluster interaction using lumped parameter models: a case study of Sichuan University Wangjiang Campus buildings. Bull Earthq Eng 19(11):4289–4310

Zhang X, Far H (2021) Effects of dynamic soil–structure interaction on seismic behaviour of high-rise buildings. Bull Earthq Eng, 1–25